

Modelling and Simulation of a Railgun Powered by a Capacitor Bank

S.G. Tatake, K.J. Daniel, A.A. Ghosh, K.P. Tokekar, K.R. Rao and I.I. Khan

Armament Research & Development Establishment, Pune-411021

ABSTRACT

A railgun powered by a capacitor bank was developed to launch hypervelocity projectiles. The efficiency of the gun to a large extent will determine its feasibility for weapon applications. A simulation code was developed to predict the performance of the railgun. The railgun has been modelled as a time-varying impedance to determine the currents and the voltages from the power source. In the railgun circuit the currents and the voltages are of the order of hundreds of kiloamperes. Even very low impedances of the order of milli-ohm and micro-henry are substantial sources of energy losses. The measured and simulated currents at peak values agree with in 10%, validating the model. The simulation code accurately predicts the energy distribution in the system. Maximization of the projectile energy leads to improved and efficient designs. The simulation also leads to the optimized launcher pressure and payload velocity.

NOMENCLATURE

C_n	capacitance of capacitors for module _n	R_4	resistance of transmission line from pulse forming coil to railgun
R_n	resistance of capacitors for module _n	R_{n1}	$R_n + R_{trans1n} + R_{mswn}$
L_n	inductance of capacitors for module _n	L_{n1}	$L_n + L_{trans1n} + L_{mswn}$
L_{coiln}	inductance of pulse forming Coil in module _n	R_{n3}	$R_{coiln} + R_4$
R_{coiln}	resistance of pulse forming coil in module _n	L_{n3}	$L_{coiln} + L_4$
L_{mswn}	inductance of the main switch in module _n	R_{ext1}	R_{n1} for $n=1$ to 3
R_{mswn}	resistance of the main switch in module _n	L_{ext1}	L_{n1} for $n=1$ to 3
L_{crbn}	inductance of the crowbar switch in module _n	R_{ext2}	$R_4 + R_{n3}$ for $n=1$ to 3
R_{crbn}	resistance of the crowbar switch in module _n	L_{ext2}	$L_4 + L_{n3}$ for $n=1$ to 3
$L_{trans1n}$	inductance of transmission line from capacitors to main switch in module _n	$R_{var}(t)$	resistance of rail at time t . Also defined as $R_{rail}(t)$ or R_5
$R_{trans1n}$	resistance of transmission line from capacitors to main switch in module _n	$L_{var}(t)$	inductance of rail at time t . also defined as $L_{rail}(t)$ or L_5
$L_{trans2n}$	inductance of transmission line from main switch to pulse forming coil in module _n	EC	energy in capacitors
$R_{trans2n}$	resistance of transmission line from main switch to pulse forming coil in module _n	E_{proj}	energy of projectile
L_4	inductance of transmission line from pulse forming coil to railgun	E_{arc}	energy of arc
		ER_{rail}	energy in resistance of rails
		EL_{rail}	energy in inductance of rails
		ER_{crb}	energy of resistance of crowbar switches

Received 27 July 1992

EL_{crb}	energy of inductance of crowbar switches
ER_{ext1}	energy in R_{ext1}
ER_{ext2}	energy in R_{ext2}
EL_{ext1}	energy in L_{ext1}
EL_{ext2}	energy in L_{ext2}
Area	bore area
m	mass of projectile
t	time
$s(t)$	displacement of the projectile at time t
$v(t)$	velocity of the projectile at time t
$a(t)$	acceleration at time t
$p(t)$	pressure at time t
$f(t)$	force at time t
	inductance of the rails
	inductance per unit length of rail (derivative of inductance wrt length of rails)
	current through the railgun
i_m	current in a circuit loop
i_m'	first derivative of i_m with respect to time
i_m''	second derivative of i_m with respect to time
m	takes values 1 to 6 as defined in Fig. 2
n	takes values 1, 2 and 3. It represents the modules in the part of the railgun circuit as shown in Fig. 2.
V_{crbn}	voltage across L_{crbn} and R_{crbn}
V_{peakn}	charging voltage across capacitor C_n

1. INTRODUCTION

A facility was developed to launch hypervelocity projectiles using electromagnetic energy. The projectiles are launched using a railgun. The railgun consists of two parallel rails and a conducting metallic foil placed behind the insulating projectile. When a high current flows through the rails, the foil explodes and forms a plasma armature. The railgun currents are in the region of hundreds of kiloamperes. The Lorentz force generated accelerates the projectile¹.

$$f = 0.5 * I * I' \tag{1}$$

A railgun powered by a capacitor bank is used to launch projectiles at hypervelocities^{2,4}. The railgun setup is shown in Fig. 1. The capacitor energy is switched into the railgun by high power ignitrons. Additional

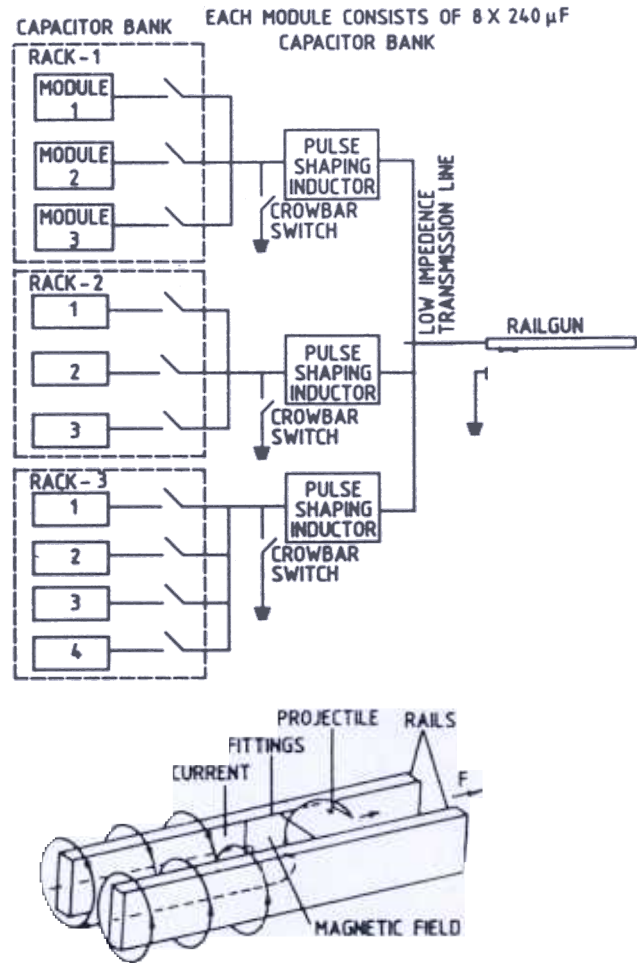


Figure. 1 A railgun powered by a capacitor bank.

high power ignitrons are used to crowbar the capacitors out of the circuit when the current is maximum. There was a need to predict how changes in the experimental setup would affect the final projectile velocities. To achieve this end, a model was developed by the authors. This paper discusses the model and its applications.

2. MODEL

A model of the railgun circuit with the capacitor bank as the power source is developed to predict the performance of the railgun, as shown in Fig. 2. The modelling of the various circuit elements are briefly described in the following.

2.1 Railgun

The railgun is modelled as a variable resistance $R_{rail}(t)$ in series with a variable inductance, $L_{rail}(t)$.

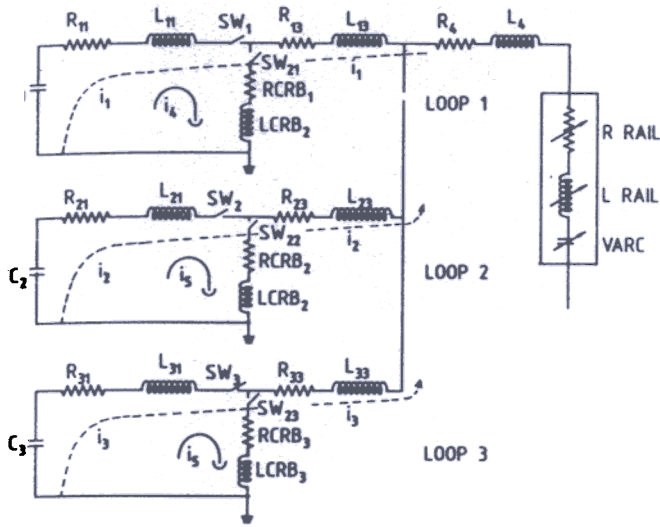


Figure 2. A model of the railgun circuit powered by the capacitor bank.

2.2 Projectile

The projectile itself is modelled as a constant mass and the drag force is modelled as a fraction of the accelerating force. The effective accelerating forces are a fraction of the total accelerating forces. This fraction is defined as the friction factor, (*F*-factor), given by

$$F\text{-factor} = (1\text{-drag}) \quad (2)$$

2.3 Plasma arc

The plasma arc is modelled as a voltage V_{arc} . The values are obtained experimentally.

2.4 Current Switch

The ignitron which is the current switch has been modelled (i) as a fixed resistance in series with a fixed inductance, and (ii) as a constant arc voltage drop.

2.5 Transmission Lines

The transmission lines are modelled as fixed inductances in series with fixed resistances. The capacitors are stacked in three racks having its own ignitrons as the current switches and crowbar switches, as shown in Fig. 1. The crowbar switches are initially off and at the peak of the current are simultaneously operated.

3. SYSTEM DIFFERENTIAL EQUATIONS

Figure 2 shows the circuit diagram which is used to derive the equations that determine the currents

through the railgun circuit. Before the current is crowbarred there exist three 2nd-order simultaneous differential equations. After the current is crowbarred there exist six 2nd order simultaneous differential equations. The equation for the current, through the part of the railgun circuit shown as LOOP1 in Fig. 2, prior to the crowbar is as follows.

$$\begin{aligned} & (R_{11}+R_{13}+R_4 + R_5 + \frac{dL_5}{dt})i_1 + \\ & (R_4+R_5 + \frac{dL_5}{dt})i_2 + (R_4+R_5 + \frac{dL_5}{dt})i_3 \\ & + (L_{11}+L_{13}+L_4+L_5) \frac{di_1}{dt} + (L_4+L_5) \frac{di_2}{dt} \\ & + (L_4+L_5) \frac{di_3}{dt} + \frac{i_1 dt}{C_1} - V_{arc} - V_{msw1} = 0 \end{aligned} \quad (3)$$

Differentiating the above equation and assuming that V_{arc} and V_{msw1} are constants, we get

$$\begin{aligned} & (L_{11}+L_{13}+L_4 + \\ & \frac{dL_5}{dt})i_1 + (L_4+L_5)i_2 + (L_4+L_5)i_3 + \\ & (R_{11}+R_{13}+R_4+R_5 + 2 \times \frac{dL_5}{dt})i_1 + (R_4 + R_5) + 2 \times \\ & \frac{dL_5}{dt})i_2 + (R_4 + R_5) + 2 \times \frac{dL_5}{dt})i_3 + \\ & (1 + \frac{dR_5}{dt} + \frac{d^2 L_5}{dt^2})i_1 + \\ & (\frac{dR_5}{dt} + \frac{dL_5}{dt^2})i_2 + (\frac{dR_5}{dt} + \frac{d^2 L_5}{dt^2})i_3 = 0 \end{aligned} \quad (4)$$

This can also be represented as

$$\begin{aligned} & A_{11}i_1 + A_{12}i_2 + A_{13}i_3 = \\ & B_{11}i_1 + B_{12}i_2 + B_{13}i_3 + C_{11}i_1 + C_{12}i_2 + C_{13}i_3 \end{aligned}$$

Similar equations for the currents can be determined for LOOP 2 and LOOP 3. After the current is crowbarred there exist 6 loops the equations for which can be similarly written. The matrix notations for these equations are given by Eqns (6) & (7). The elements

of the matrix are the coefficients of the corresponding differential terms of the equations.

$$A1 \begin{bmatrix} i_1 \\ i_2 \\ i_3 \end{bmatrix} = B1 \begin{bmatrix} i_1 \\ i_2 \\ i_3 \end{bmatrix} + C1 \begin{bmatrix} i_1 \\ i_2 \\ i_3 \end{bmatrix} \quad (6)$$

$$A2 \begin{bmatrix} i_1 \\ i_2 \\ i_3 \\ i_4 \\ i_5 \\ i_6 \end{bmatrix} = B2 \begin{bmatrix} i_1 \\ i_2 \\ i_3 \\ i_4 \\ i_5 \\ i_6 \end{bmatrix} + C2 \begin{bmatrix} i_1 \\ i_2 \\ i_3 \\ i_4 \\ i_5 \\ i_6 \end{bmatrix} \quad (7)$$

A_1 , B_1 and C_1 are 3×3 matrices and A_2 , B_2 and C_2 are 6×6 matrices. The values of the resistance and inductance of the transmission lines are obtained from the dimensions and the properties of the materials.

3.1 Solution

The elements of the matrices are substituted in the sets of 6 and 7 and after matrix inversion the following two equations are obtained.

$$\begin{bmatrix} i_1 \\ i_2 \\ i_3 \end{bmatrix} A^{-1} B1 \begin{bmatrix} i_1 \\ i_2 \\ i_3 \end{bmatrix} + A1^{-1} C1 \begin{bmatrix} i_1 \\ i_2 \\ i_3 \end{bmatrix} \quad (8)$$

$$\begin{bmatrix} i_1 \\ i_2 \\ i_3 \\ i_4 \\ i_5 \\ i_6 \end{bmatrix} A2^{-1} B2 \begin{bmatrix} i_1 \\ i_2 \\ i_3 \\ i_4 \\ i_5 \\ i_6 \end{bmatrix} + A2^{-1} C2 \begin{bmatrix} i_1 \\ i_2 \\ i_3 \\ i_4 \\ i_5 \\ i_6 \end{bmatrix} \quad (9)$$

Equations (8) and (9) are further reduced to first order differential equations. The number of equations double after the reduction. The solution is obtained

numerically using the fifth-order Runge-Kutta (Butcher) method. The time-dependent parameters are calculated at each step and substituted into the equation. Matrix inversion is done at each step before the Runge-Kutta method is applied to solve these equations. This is essential as some of the elements of A_1 and A_2 are time dependent. Initially Eqn (8) is used and after crowbarring Eqn (9) is used. The initial values for Eqn (8) are taken as

$$i = 0 \quad n = 1,2,3$$

$$i_n = V_{peakn} / (L_4 + L_{n1} + L_{n3}) \quad n=1,2,3$$

The initial values of i_n and i_n' ($n=1,2,3$) for Eqn (9) are taken from the results of Eqn (8) at the point of crowbarring.

The initial values of i_n ($n = 4,5,6$) for Eqn (9) are taken as zero. The values of the currents in the crowbar loop

$$i_n' = V_{crbn} / L_{crbn} \quad n=4,5,6$$

The current data are used to derive other significant parameters like the displacement, velocity and acceleration of the projectile calculated from Eqns (10-14).

$$s(t) = [l/(2 * m)] * \int \int i^2 dt \quad (10)$$

$$v(t) = [l/(2 * m)] * \int i^2 dt \quad (11)$$

$$a(t) = [l/(2 * m)] * i^2 \quad (12)$$

$$p(t) = [l/(2)] * i^2 / Area \quad (13)$$

$$f(t) = [l/(2)] * i^2 \quad (14)$$

Table 1 gives the summarizes the results obtained from the simulation code for a typical railgun setup.

The software code uses the values of the current to estimate the energy distribution in the railgun circuit. The energy supplied to the launcher is given by

$$E_{launch}(t) = ER_{rail}(t) + EL_{rail}(t) + E_{arc}(t) + E_{proj}(t) \quad (15)$$

The energy delivered to the projectile is given by

$$E_{proj}(t) = (1/2) * m * [v(t)]^2$$

$$\text{Launcher efficiency} = E_{proj} / E_{launch} \quad (17)$$

$$\text{System efficiency} = E_{proj} / E_{total} \quad (18)$$

The software was coded in Pascal with about 1000 lines of code.

4. USE OF THE COMPUTER MODEL

4.1 Design Criteria

The software package predicts the displacement

Table 1. The summary of the results obtained from the simulation code for a typical railgun setup

<i>Capacitor Bank Details</i>			
Capacitance of capacitor bank	0.0192	F	
Charging voltage :	4500	V	
Energy of The capacitor bank	194.40	kJ	
<i>Railgun Projectile & Barrel Details</i>			
Mass of the projectile :	3.30	g	
Friction factor :	1.00		
Arc voltage across railgun :	200.00	V	
Inductance per unit length :	0.40	μ H	
Resistance per unit length :	0.106	milli-ohm	
<i>Railgun Circuit Parameters</i>			
L_{ext1} :	0.50	μ H	
R_{ext1} :	0.50	milli-ohm	
L_{ext2} :	2.00	μ H	
R_{ext2} :	2.00	milli-ohm	
Results			
<i>For 1 m Railgun</i>		<i>For 2 m Railgun</i>	
Time	: 860.00 μ s	Time	1160.0 μ s
Current	: 209.87 kA	Current	122.07 kA
Velocity	: 2.92 km/s	Velocity	3.41 km/s
Displacement	: 1.04 m	Displacement	2.01 m
Force	: 8.81 kN	Force	2.97 kN
Pressure	: 61.18 MPa	Pressure	20.69 MPa
<i>Peak Values</i>			
Time	: 665.00 μ s		
Peak current	: 290.0 kA		
Peak pressure	: 117.58 MPa		

velocity and the acceleration of the projectile at different increments of time. The allowable peak forces and pressures in the launcher and the projectile could be estimated and materials chosen accordingly. An increase in the inductance at the railgun end stretches the current pulse and leads to lower peak currents, forces and pressures respectively. Lower forces, in turn, reduce the damage to the railgun and the projectile. More energy is delivered to the projectile as the launching forces last for a longer time. Railguns were designed with lengths that could suitably utilise the entire forces generated from the stretched current pulses.

4.2 Efficiency

There is a need to reduce the resistances and inductances of transmission lines to minimize the energy losses in the circuit and maximize the projectile energy. This has led to the use of parallel-plate, sandwiched, low inductance transmission lines. A typical output showing the energy distribution at 1 m from the rail is

Table 2. The energy distribution in a railgun at projectile exit for a 1 m railgun

Symbol	Energy %
E_{proj}	5.59
E_{arc}	17.50
ER_{rail}	0.57
EL_{rail}	2.48
ER_{crb}	0.00
EL_{crb}	0.00
ER_{ext2}	43.53
EL_{ext2}	12.75
ER_{ext1}	6.25
EL_{ext1}	11.08
EC	0.24

given in Table 2. The inductance per unit length of the rails needs to be increased to maximize the energy inside the launcher. This leads to the design of augmented rails to increase the launcher forces and ultimately to raise the projectile velocity⁶.

5. DATA ACQUISITION AND MODEL VALIDATION

The performance of the model was validated using a multi-channel data acquisition system⁷. Rogowski coils were used to measure the currents⁸. The measured current values and the simulated current values [along with the results derived from Eqns (10-14)] were compared to validate this computer model. The difference between the measured and simulated current

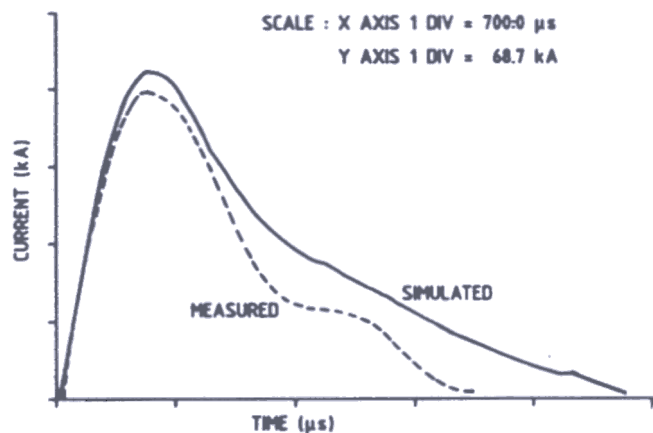


Figure 3. The measured and simulated current waveform for a typical railgun circuit configuration.

values was within 10 per cent at peak values (Fig. 3). The breech and the muzzle voltages were monitored and, along with the current signals, were used to estimate the arc voltage and resistance. The energy of the launcher and the gun efficiency were computed. The projectile exit at the muzzle was also indicated on the muzzle voltage signal. Magnetic flux probes were used to obtain the displacement of the plasma armature which leads to the in-bore velocity and the acceleration of the projectile⁹. The velocity and the current signal obtained using Eqn (9), help in estimating the inductance per unit length of the railgun—a useful input to the simulation code. The pulses from the shorting screens were used to monitor the velocity outside the bore of the railgun.

6. CONCLUSION

The results obtained from the computer simulation and the results from the experimental measurements were in fair agreement, indicating that the basis of the model is sound. This was of immense help in making modifications to our experimental setup with a view to

maximize projectile velocities and railgun efficiency. The model however does not take into account skin effects. The structure of the plasma has also not been considered in this model, due to lack of diagnostic techniques to study and monitor the plasma behaviour. The switches need to be modelled as a variable voltage with data obtained from experiments. The variations in results could be attributed to the above shortcomings leading to inaccuracies. Further refinement of this software code, supported by additional experiments will lead to even firmer foundation for future prediction of railgun performance and potentials.

ACKNOWLEDGMENTS

We thank Major Gen D Kapil, Director of Armament Research and Development Establishment, Pune, for giving us permission to present this paper. We are indebted for the facilities that were made available to us in this Establishment. The authors are grateful to all the members of the trial team who were instrumental for the completion of this work.

REFERENCES

1. Weeks, D.A.; Weldon, W.F. & Zowarka Jr, R.C. Plasma armature railgun launcher simulations at the University of Texas at Austin. *IEEE Trans. Magnetics*, 1989, **25**(1), 580-86.
2. Rashleigh, S.C. & Marshall, R.A. Electromagnetic acceleration of macroparticles to high velocities *J. App. Phys.*, 1980, **49**, 2540.
3. Hawake, R.S.; Brooks, A.L.; Deadrick, F.J.; Schudder, J.K.; Fowler, C.M.; Caird, R.S. & Peterson, D.R. Results of railgun experiments powered by magnetic flux compression generators. *IEEE Trans. Magnetics*, 1982, **Mag-18**, 82-93.
4. Tataka, S.G.; Daniel, K.J.; Ghosh, A.A.; Rao, K.R.; Tokekar, K.P. & Khan, I.I. To establish technique for launching hypervelocity projectiles. March 1991, *ARDE Closing Rep. No. 892*.
5. Clark, G.A. & Bedford, A.J. Performance results of a small caliber electromagnetic launcher. *IEEE Trans. Magnetics*, 1984, **Mag-20**(2), 276-79.
6. Mاريو, T.; Fujioka, K.; Nagaoka, K.; Akihiro, O.; Kazunari, I. & Neimoto, K. Electromagnetic acceleration studies with augmented rails. *IEEE Trans. Magnetics*, 1991, **27**(1), 65-67.

7. Tatake, S.G.; Daniel, K.J.; Ghosh, A.A.; Rao, K.R.; Tokekar, K.P. & Khan, I.I. Diagnostics for an electromagnetic propulsion system. Paper presented at the All India Conference on Applied Instrumentation, Rorkee, 14-15 February, 1992. pp. 275-78.
8. Pellinen, D.G.; Di Cpana, M.S.; Sampayan, S.E.; Gerbracht H. & Wang, M. Rogowskii coil for measuring fast high level pulsed currents. *Rev. Sci. Instrum.*, 1980, **51**, 1535-39.
9. Bauer, D.P. & Barber, J.P. In-bore railgun projectile velocity. *IEEE Trans. Magnetics*, 1986, **Mag-22(6)**, 1395-98.